

Optics Letters

Efficient $\text{Yb}^{3+}:\text{CaGdAlO}_4$ bulk and femtosecond-laser-written waveguide lasers

KORE HASSE,^{1,*} THOMAS CALMANO,^{1,2} BASTIAN DEPPE,^{1,2,3} CHRISTOPH LIEBALD,⁴ AND CHRISTIAN KRÄNKEL^{1,2}

¹Institut für Laser-Physik, Universität Hamburg, Luruper Chaussee 149, 22761 Hamburg, Germany

²The Hamburg Center for Ultrafast Imaging, Universität Hamburg, Luruper Chaussee 149, 22761 Hamburg, Germany

³Center for Free-Electron Laser Science, DESY, Hamburg, Notkestraße 85, 22761 Hamburg, Germany

⁴FEE, Struthstraße 2, 55743 Idar-Oberstein, Germany

*Corresponding author: khasse@physnet.uni-hamburg.de

Received 1 June 2015; revised 2 July 2015; accepted 3 July 2015; posted 6 July 2015 (Doc. ID 241973); published 24 July 2015

We report on, to the best of our knowledge, the first fs-laser-written waveguide laser in $\text{Yb}^{3+}:\text{CaGdAlO}_4$ (Yb:CALGO). With Yb:CALGO crystals grown in our labs, we obtained a slope efficiency of 69% and up to 2.4 W of continuous wave (cw) output power in a waveguide-laser configuration. Moreover, bulk laser experiments with Yb:CALGO were performed, and slope efficiencies up to 73%, optical-to-optical efficiencies of 65%, and maximum cw output powers of 3.3 W were reached. These are the highest efficiencies in the laser configuration with Yb:CALGO. © 2015 Optical Society of America

OCIS codes: (140.3570) Lasers, single-mode; (230.7380) Waveguides, channeled.

<http://dx.doi.org/10.1364/OL.40.003552>

The disordered crystal Yb:CALGO is a unique material for the generation of ultrashort pulses. It provides wide emission bands comparable to those of Yb^{3+} -doped glasses combined with much better thermo-mechanical properties [1]. Since its first demonstration as a laser material [2], pulses as short as 32 fs have been realized with a Kerr-lens mode-locked Yb:CALGO oscillator [3], and pulse durations of 40 fs were obtained with semiconductor saturable absorber-mirror (SESAM) mode locking [4].

Recently, Yb:CALGO crystals grown in our labs allowed for significantly higher efficiencies in the thin disk laser setup than previously reported [5] for this material and a wide wavelength tuning range [6].

The femtosecond-laser (fs-laser) writing of waveguides into crystalline materials has been shown to be a very versatile method for the fabrication of efficient waveguide lasers in different materials [7,8]. Similar waveguides in ion-exchanged glass have been utilized for GHz-mode-locked fs-waveguide lasers [9]. Cw mode-locked laser operation in fs-laser-written waveguides was first realized in a fiber-extended cavity [10]. Very recently, the first mode-locked Nd:YAG fs-laser-written

waveguide laser operating at 11-GHz repetition rate, an average output power of 12 mW, and 16-ps pulse duration was realized utilizing graphene as the saturable absorber [11]. Our approach is to combine the unique features of Yb:CALGO for the generation of ultrashort pulses with the benefits of the waveguide geometry. With a fs-laser-written mode-locked Yb-doped CALGO waveguide laser it should be possible to achieve fs pulses at repetition rates in the order of GHz, too. However, lower thresholds and higher output power can be expected due to the higher gain cross sections and better thermo-mechanical properties of Yb^{3+} in CALGO compared to Yb-doped glasses.

In this Letter, we report on the realization of the first (to the best of our knowledge) fs-laser-written waveguide laser in Yb:CALGO and on the spectroscopy and highly efficient bulk laser operation of this material under pumping with an optically pumped semiconductor laser (OPSL).

The Czochralski growth of the Yb:CALGO crystals used in the experiments is described in [6]. The doping concentration of Yb^{3+} in the melt was 10%. An Ir-wire was used as seed. Laue measurements revealed an angle of $\sim 72^\circ$ between the growth direction of the crystal and the c axis. In earlier growth runs, crystal growth was also observed perpendicular to the optical axis. By energy-dispersive x-ray spectroscopy (EDX), the Yb^{3+} -concentration was determined to be $(6.6 \pm 0.8) \times 10^{20} \text{ cm}^{-3}$ at the top and $(9.0 \pm 0.4) \times 10^{20} \text{ cm}^{-3}$ at the bottom of the boule. At a cation density of $1.25 \times 10^{22} \text{ cm}^{-3}$ in Yb:CALGO with respect to the Gd sites, this corresponds to a doping concentration of $(5.3 \pm 0.6)\%$ and $(7.2 \pm 0.3)\%$, respectively, and results in a segregation coefficient of ~ 0.5 .

Due to this low segregation coefficient, there was some ambiguity about the cross-section values for Yb:CALGO in the past, as possibly the doping concentration in the melt was taken for their determination [2,12,13]. For this reason, we thoroughly refined the absorption and emission cross sections.

Yb:CALGO has a uniaxial tetragonal crystal structure. Hence the cross sections were determined for electrical field vectors parallel and perpendicular to the optical axis. The

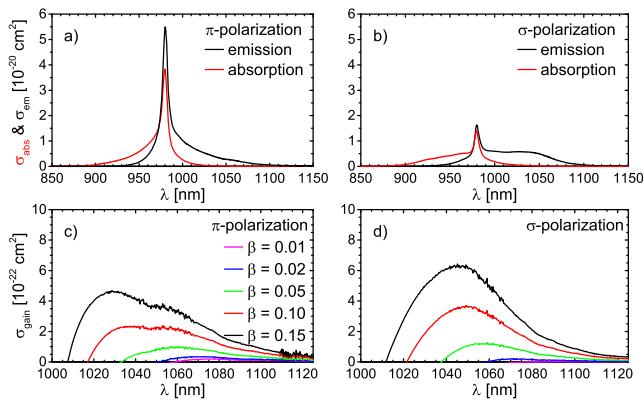


Fig. 1. (a), (b) Polarized absorption (σ_{abs}) and emission (σ_{em}) cross sections of Yb:CALGO. (c), (d) Corresponding gain cross sections (σ_{gain}) for different inversion levels β , as a function of wavelength λ .

absorption cross sections were determined from transmission measurements utilizing the Beer–Lambert law and the measured doping concentrations. The resulting peak values of $3.8 \times 10^{-20} \text{ cm}^2$ in π - and $1.4 \times 10^{-20} \text{ cm}^2$ in σ -polarization were observed at a wavelength of 979.6 nm (cf. Fig. 1). The peak values in σ -polarization are about 11% higher than the values in [12], and the anisotropy between π - and σ -polarization of 2.7 is somewhat smaller than the value of 3 reported there. It should be noted that only the first deviation may arise from the error in the determination of the doping concentration. However, as our crystals were oriented by Laue-diffraction, and the doping concentration was determined by EDX resulting in segregation coefficients that are in good agreement with our previous measurements, we are very confident that our values are precise.

Due to the quasi-three-level scheme of Yb^{3+} , the fluorescence spectra are biased by reabsorption in the respective wavelength range. Therefore, we used a combination of the McCumber-relation [14] and the Füchtbauer–Ladenburg method (FL) as described in [15] for the determination of the emission cross sections. Because of the disordered nature of the CALGO host, where Yb^{3+} occupies the C_{4V} site shared by Ca^{2+} and Gd^{3+} ions [16], the energetic position of the Stark levels cannot be measured properly. Hence the spectra resulting from the McCumber relation were calibrated with the FL-emission cross sections at 1050 nm, where no reabsorption is expected. The absorption, emission, and gain cross-section spectra are shown in Fig. 1. It should be noted that the cross sections, in particular in π -polarization, are much higher than the values reported in [2] and differ significantly from those in [12]. We determined an emission cross section of $5.5 \times 10^{-20} \text{ cm}^2$ in π -polarization and $2.0 \times 10^{-20} \text{ cm}^2$ in σ -polarization for the zero-phonon line transitions around 980 nm. For inversion levels >0.025 , the gain cross sections are higher in σ -polarization in the range of possible laser action around 1040 nm [see Figs. 1(c) and 1(d)]. In this range, the emission cross-section spectra are very broad and nearly unstructured in both polarizations. This property favors the broad tunability and short pulse duration in mode-locked laser operation [4–6,17]. The fluorescence lifetime was determined by

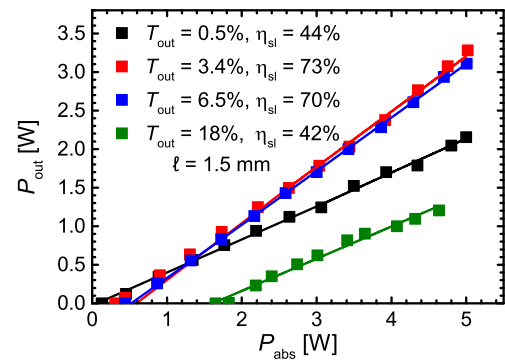


Fig. 2. Laser characteristics and linear fits (straight lines) of an OPSEL-pumped 1.5-mm Yb(5.4%):CALGO crystal. The cw laser output power P_{out} is plotted against the absorbed pump power P_{abs} for different output coupler transmissions T_{out} .

the pinhole method [18,19]. For different crystals with doping concentrations between 4.9% and 10%, it did not change significantly and was always in the order of $(445 \pm 10) \mu\text{s}$, comparable to the results in [12].

Bulk laser experiments were performed with a 1.5-mm-long $\sim 5.4\%$ Yb^{3+} -doped sample in a near-concentric resonator with a length of 190 mm and radii of curvature of 100 mm of input coupling and output coupling mirrors. The laser crystal was placed on a water-cooled copper heat sink. A pump source, an OPSEL with $\sim 6 \text{ W}$ of maximum output power at the pumping wavelength of 980.4 nm, was applied. The pump beam was polarized parallel to the optical axis and focused with a lens of a focal length of 75 mm into the crystal. The cw laser output was σ -polarized in all experiments, corresponding to the higher gain cross sections in this polarization. For output coupling, different mirrors with transmissions for the laser wavelength between 0.2% and 18% were used. The best laser performance was obtained at an output coupler transmission of 3.4%. In this case, the laser delivered a maximum output power of 3.3 W at 5.0 W of absorbed pump power and a slope efficiency of 73%. This is, to the best of our knowledge, the highest slope efficiency reached with Yb:CALGO in a bulk laser configuration. The optical-to-optical efficiency was as high as 60% with respect to the incident pump power. The fraction of absorbed pump power was assumed to be constant from the laser threshold on. Factoring in a double-pass of the pump light and the Fresnel reflection at both crystal end faces resulted in an absorption efficiency of 92% and thus 65% of optical-to-optical efficiency with respect to the absorbed pump power for the laser with the highest slope efficiency. In all other bulk experiments, the fraction of absorbed pump power exceeded 75%. The laser wavelength varied between 1095 nm with a highly reflective output coupling mirror and 1043 nm at 18% transmission. This is consistent with the spectroscopic investigations (cf. Fig. 1). Laser characteristics for four different output couplers are depicted in Fig. 2. It should be noted that the laser thresholds are comparably high for a laser in this resonator configuration. This is attributed to the length of the crystal. It corresponds to ~ 5 absorption lengths, leading to a higher pump power needed to bleach the reabsorption at the laser wavelength. For thinner crystals, we could observe lower laser thresholds at somewhat

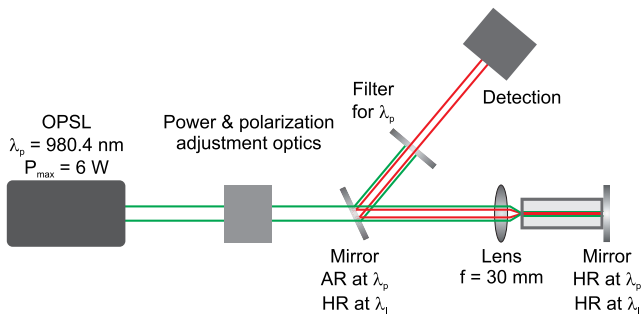


Fig. 3. Schematic of the waveguide laser setup.

lower laser efficiencies. However, the large thickness of our samples is advantageous for future bulk-mode-locking experiments in a configuration similar to the ones in [20,21]. These results show that the Yb:CALGO crystals grown in our laboratory have very good properties as laser materials in bulk laser configuration. Therefore, we performed further experiments on fs-laser-written waveguides.

The femtosecond-laser writing technique for the fabrication of waveguides is based on modification of the crystal material in the laser focus due to nonlinear absorption effects [22].

In crystalline materials, often so-called type II modifications are employed, in which waveguiding is enabled by stress-induced refractive-index change in the material surrounding the modifications [7,8]. In this way, efficient waveguiding is possible, for example, between two parallel tracks. To produce such waveguides, a chirped-pulse amplification femtosecond-laser system was used. The system provides 150-fs pulses at a repetition rate of 1 kHz and pulse energies up to 1 mJ at a wavelength of 775 nm. The setup and preparation of the waveguides is described in detail in [7]. For the writing process, the pulses were focused $\sim 340 \mu\text{m}$ below the surface of the crystal with a fully illuminated aspheric lens of a focal length of 4.51 mm and a numerical aperture of 0.55. The sample was moved transversally to the incident beam by a motorized three-dimensional positioning system with a velocity of $25 \mu\text{m/s}$.

We inscribed tracks in three different samples with track orientations parallel and perpendicular to the growth direction [black arrow in Fig. 4(a)]. The lengths of the samples were about 1 cm, and the doping concentration was 7.2% with respect to the Gd sites. Various double tracks with track distances between 18 and $28 \mu\text{m}$ were inscribed into all samples using pulse energies between 0.45 and $2.3 \mu\text{J}$. Tracks were also written with the fs laser being polarized in the writing direction, perpendicular to the writing direction, or circularly polarized.

The induced refractive-index change apparently depends on the orientation of the tracks with respect to the crystallographic axes. Good waveguiding could only be obtained for the orientation of the waveguides shown in Fig. 4(a).

According to further Laue measurements, the waveguides are perpendicular to the set of symmetrically equivalent lattice planes (1 1 14), which is in good agreement with the unexpected angle of $\sim 72^\circ$ between the c axis and the growth direction mentioned previously. A minor deviation from the angle of 90° between (1 1 14) and the other planes in Fig. 4(a) is attributed to inaccuracies during the preparation of the sample.

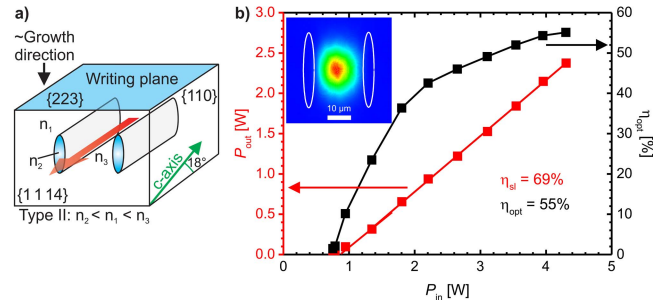


Fig. 4. (a) Schematic of the orientation of waveguide laser crystal. (b) Characteristics of the waveguide laser with the mode-profile measured at 96 mW as inset. The cw output power P_{out} and optical efficiency η_{opt} are plotted against the incident power P_{in} .

The induced refractive-index change also depended on the polarization of the fs-laser beam with respect to the waveguide. A polarization of the fs-laser beam perpendicular to the writing direction allowed for the best results. The writing parameters that proved to be best were a track distance of $25 \mu\text{m}$ and a pulse energy of $1.5 \mu\text{J}$. With these waveguides, we achieved good light confinement and losses of $\sim 1.1 \text{ dB/cm}$ (22% for the 9-mm-long waveguide) at 633 nm.

As often observed in such type II double track waveguides, only one polarization direction is guided. However, in this case, the polarization of the guided light was tilted by $\sim 10^\circ$ with respect to the normal vector of the writing plane (i.e., the growth direction). Such a behavior has previously not been observed in fs-laser-written waveguides and is attributed to the unusual orientation of the waveguides with respect to the crystallographic axes.

Laser operation could not be obtained without any external mirrors, as was reported for waveguide lasers in other crystals [7]. Therefore, a highly reflective mirror was attached to the end facet of the waveguide crystal. The laser setup is depicted schematically in Fig. 3. Similar performance could also be obtained with the mirror attached to the incoupling facet of the waveguide. The pump beam was focused with a lens with a focal length of 30 mm onto the entrance face of the waveguide. The same OPSP was used as a pump source. The waveguide laser characteristics are depicted in Fig. 4(b).

In this configuration we achieved a maximum cw output power of 2.4 W at an incident pump power of 4.4 W. The laser threshold was 0.76 W. This results in an optical efficiency of 55%. The slope efficiency was as high as 69% with respect to the Fresnel-corrected incident pump power. Considering the incoupling efficiency of the pump into the waveguide, which is about 90% for this setup, the slope efficiency of 76% is even higher than in the bulk laser experiments. The laser wavelength varied between 1029.6 and 1041.5 nm depending on the alignment of the mirror on the end facet, i.e., the Fabry–Perot-type effect due to the air gap between waveguide and mirror. These short wavelengths point toward a higher inversion level in the waveguide compared to the bulk laser experiments (cf. Fig. 1), which is reasonable regarding the high output coupling and losses. We measured a decreasing mode diameter with increasing laser output power. The $1/e^2$ diameter of the mode

changed from $19 \times 25.4 \mu\text{m}$ at 96 mW to $17 \times 23 \mu\text{m}$ at 1.84 W of output power in the waveguide presented here. An even stronger effect was observed in a slightly longer waveguide with similar fabrication parameters. This is attributed to an increased refractive-index gradient due to thermal effects, which at this extent has not been observed in other fs-laser-written waveguides. The mode-profile for an output power of 96 mW is shown exemplarily in the inset of Fig. 4. The measured M^2 -value was 1.1. The high slope efficiency of 69% makes this Yb:CALGO waveguide laser one of the most efficient fs-laser-written solid-state waveguide lasers. In terms of maximum output power, it was only surpassed by Yb:YAG waveguides [7].

In conclusion, we refined the absorption and emission cross sections of Yb:CALGO. With crystals grown in our lab, we realized a bulk laser with a very high slope efficiency of 73% and, to the best of our knowledge, the first waveguide laser with a slope efficiency of 69% and 2.4 W of output power in Yb:CALGO. The broad wavelength range of the waveguide laser should be advantageous for future mode-locked Yb:CALGO waveguide lasers.

Funding. Deutsche Forschungsgemeinschaft (DFG) (CA 1380/1-1).

REFERENCES

1. Y. Zaouter, J. Didierjean, F. Balembois, G. Lucas Leclin, F. Druon, P. Georges, J. Petit, P. Goldner, and B. Viana, *Opt. Lett.* **31**, 119 (2006).
2. J. Petit, P. Goldner, and B. Viana, *Opt. Lett.* **30**, 1345 (2005).
3. P. Sévillano, P. Georges, F. Druon, D. Descamps, and E. Cormier, *Opt. Lett.* **39**, 6001 (2014).
4. A. Agnesi, A. Greborio, F. Pirzio, G. Reali, J. Aus der Au, and A. Guandalini, *Opt. Express* **20**, 10077 (2012).
5. S. Ricaud, A. Jaffres, K. Wentsch, A. Suganuma, B. Viana, P. Loiseau, B. Weichelt, M. Abdou-Ahmed, A. Voss, T. Graf, D. Rytz, C. Hönninger, E. Mottay, P. Georges, and F. Druon, *Opt. Lett.* **37**, 3984 (2012).
6. K. Beil, B. Deppe, and C. Kränkel, *Opt. Lett.* **38**, 1966 (2013).
7. T. Calmano and S. Müller, *IEEE J. Sel. Top. Quantum Electron.* **21**, 401 (2015).
8. F. Chen and J. R. Vázquez de Aldana, *Laser Photon. Rev.* **8**, 251 (2014).
9. R. Osellame, G. Della Valle, N. Chiodo, S. L. Taccheo, O. Svelto, and G. Cerullo, *Appl. Phys. A* **93**, 17 (2008).
10. S. J. Beecher, R. R. Thomson, N. D. Psaila, Z. Sun, T. Hasan, A. G. Rozhin, A. C. Ferrari, and A. K. Kar, *Appl. Phys. Lett.* **97**, 111114 (2010).
11. A. G. Okhrimchuk and P. A. Obraztsov, *Sci. Rep.* **5**, 11172 (2015).
12. F. Pirzio, S. D. Di Dio Cafioso, M. Kemnitzer, A. Guandalini, F. Kienle, S. Veronesi, M. Tonelli, J. Aus der Au, and A. Agnesi, *Opt. Express* **23**, 9790 (2015).
13. K. Beil, B. Deppe, and C. Kränkel, *Advanced Solid-State Lasers Conference*, Paris, France, 2013, paper AF3A.1.
14. D. E. McCumber, *Phys. Rev.* **136**, A954 (1964).
15. P. H. Haumesser, R. Gaume, B. Viana, and D. Vivien, *J. Opt. Soc. Am. B* **19**, 2365 (2002).
16. H. Sawada, F. Marumo, and N. Kodama, *J. Solid State Chem.* **139**, 204 (1998).
17. D. N. Papadopoulos, F. Druon, J. Boudeille, I. Martial, M. Hanna, P. Georges, P. O. Petit, P. Goldner, and B. Viana, *Opt. Lett.* **34**, 196 (2009).
18. C. Kränkel, D. Fagundes-Peters, S. T. Friedrich, J. Johannsen, M. Mond, G. Huber, M. Bernhagen, and R. Uecker, *Appl. Phys. B* **79**, 543 (2004).
19. H. Kühn, S. T. Friedrich-Thornton, C. Kränkel, R. Peters, and K. Petermann, *Opt. Lett.* **32**, 1908 (2007).
20. M. Tokurakawa, A. Shirakawa, K. I. Ueda, H. Yagi, T. Yanagitani, A. A. Kaminskii, K. Beil, C. Kränkel, and G. Huber, *Opt. Express* **20**, 10847 (2012).
21. A. Heuer, K. Beil, and C. Kränkel, "Highly efficient cw and mode-locked OPSSL pumped Yb:Lu₂O₃-lasers," in *EPS-QEOD Europhoton Conference*, Neuchâtel, Switzerland, August 29, 2014, paper FrB-T10-05.
22. T. Gorelik, M. Will, S. Nolte, A. Tuennermann, and U. Glatzel, *Appl. Phys. A* **76**, 309 (2003).